

Supporting Information

Na_{0.86}Co_{0.95}Fe_{0.05}O₂ layered oxide as highly efficient water oxidation electrocatalyst in alkaline media

Jie Dai,[†] Yinlong Zhu,[†] Yubo Chen,[†] Wei Zhou,[†] and Zongping Shao^{*,‡,§}

[†] Jiangsu National Synergetic Innovation Center for Advanced Materials (SICAM), State Key Laboratory of Materials-Oriented Chemical Engineering, College of Chemical Engineering, Nanjing Tech University, No.5 Xin Mofan Road, Nanjing 210009, P.R. China.

[‡] Jiangsu National Synergetic Innovation Center for Advanced Materials (SICAM), State Key Laboratory of Materials-Oriented Chemical Engineering, College of Energy, Nanjing Tech University, No.5 Xin Mofan Road, Nanjing 210009, P.R. China.

[§] Department of Chemical Engineering, Curtin University, Perth, Western Australia 6845, Australia.

*To whom correspondence should be addressed.

E-mail: shaozp@njtech.edu.cn.

Tel: (+86) 25-83172256.

Fax: (+86) 25-83172242.

Experimental section

Catalyst preparation. The catalyst powders $\text{NaCo}_{1-x}\text{Fe}_x\text{O}_2$ ($x=0, 0.05, 0.1$) were prepared via a facile combined EDTA-citrate complexing sol-gel method. In a typical synthesis, the required stoichiometric transition metal nitrates (all analytical grade, Sinopharm Chemical Reagent Co., Ltd.) as raw materials were dissolved in deionized water under stirring. Then, the complexing agents of EDTA and citrate acid were poured into the obtained solution in a 1:1:2 molar ratio of total transition metal cations:EDTA:CA, followed by adding NH_3 aqueous solution to adjust the pH to 5. During the entire process, continuous stirring and heating at 90 °C were necessary to obtain a transparent gel. The resulting solid precursor was acquired by heating the gel at 250 °C for 5 h in a furnace. In the end, $\text{NaCo}_{1-x}\text{Fe}_x\text{O}_2$ powders were obtained by calcining the solid precursors at 800 °C for 5 h in air.

Material Characterizations. To determine and evaluate the crystal structure and phase purity, XRD patterns of the resultant powders were collected by X-ray powder diffraction (XRD, Rigaku Smartlab) with Cu $K\alpha$ radiation ($\lambda=1.5418 \text{ \AA}$) in the 2θ range of 10 to 90° at room temperature with a tube voltage of 40 kV, tube current of 40 mA and an interval of 0.02°. Further crystal structure parameters were explored by Rietveld refinement of the XRD

patterns, assisted by the general structure analysis system (GSAS) program and EXPGUI interface. The chemical compositions of the as-prepared samples were determined by applying inductively coupled plasma-optical emission spectrometry (ICP-OES, PerkinElmer). The specific surface areas of the catalyst powders were investigated using a nitrogen adsorption-desorption analyser (BELSORP II) and calculated by the Brunauer-Emmett-Teller (BET) method. The morphologies of the powders were inspected by using an environmental scanning electron microscope (ESEM, QUANTA-2000). The surface chemical states of the samples were obtained by X-ray photoelectron spectroscopy (XPS, PHI5000 VersaProbe spectrometer) equipped with an Al K α X-ray radiation source, where the binding energies were corrected to the adventitious C 1s peak at 284.6 eV and the data were fitted by the public software package XPSPEAK.

Electrochemical measurements. All electrochemical measurements were conducted using a typical three-electrode system, in which a platinum plate, Ag|AgCl (3.5 M KCl), and a rotating disk electrode of glassy carbon (GC-RDE, 5 mm diameter, 0.196 cm²) coated with the electrocatalyst suspension acted as the counter, reference, and working electrode, respectively. The working electrode was connected to an electrochemical workstation (PARSTAT 2273, Princeton Applied Research) and tested in O₂-saturated 0.1 M KOH electrolyte (99.99% metal purity, pH ~12.6) at room temperature. The GC substrate was pre-polished by α -Al₂O₃ (50 nm) before each test. Note that working electrodes

were fabricated in two steps: a mixture of the catalyst powder (10 mg), conductive carbon (Super P Li, 10 mg), Nafion solution (5 wt%, 100 μ L), and absolute ethanol (1 mL) were homogeneously dispersed by sonication to obtain the required electrocatalyst suspension; a 5 μ L aliquot of the resultant suspension was loaded on the surface of the GC substrate, which generated an approximate catalyst loading of 0.232 $\text{mg}_{\text{oxide}} \text{cm}^{-2}_{\text{disk}}$; and the obtained working electrode was dried for 1 h. The GC-RDE rotation speed was set at 1600 rpm to eliminate the influence of oxygen bubbles on the GC surface during electrochemical measurement. Linear sweep voltammetry was carried out at a scan rate of 5 mV s^{-1} with voltages ranging from 0.2 to 1.0 vs. Ag|AgCl (3.5 M KCl). Cyclic voltammetry measurements were carried out at a scan rate of 100 mV s^{-1} with voltages ranging from 0.2 to 0.8 vs. Ag|AgCl (3.5 M KCl). The mass activity normalized to the catalyst mass loading (MA) and specific activity normalized to the surface area (SA), shown in Fig. 2, were calculated by the following equations: $\text{MA}=\text{J}/\text{m}$ and $\text{SA}=\text{J}/(10\times\text{m}\times\text{a}_{\text{s, BET}})$, where J is the current density at $\eta=0.45$ V and m is the catalyst loading on the working electrode. All potential values were iR-corrected by the calculation: iR-corrected $E=E-iR$, where i represents the current and the electrolyte resistance R approximately equals ~ 45 ohm, measured by high-frequency AC impedance under the above-mentioned test conditions. Electrochemical impedance spectroscopy (EIS) was recorded at 0.7 V vs. Ag|AgCl (3.5 M KCl) from 10^5 to 0.1 Hz at an amplitude of 10 mV. Durability tests were measured

using the chronopotentiometry method with a current density of 5 mA cm^{-2} for 3 h.

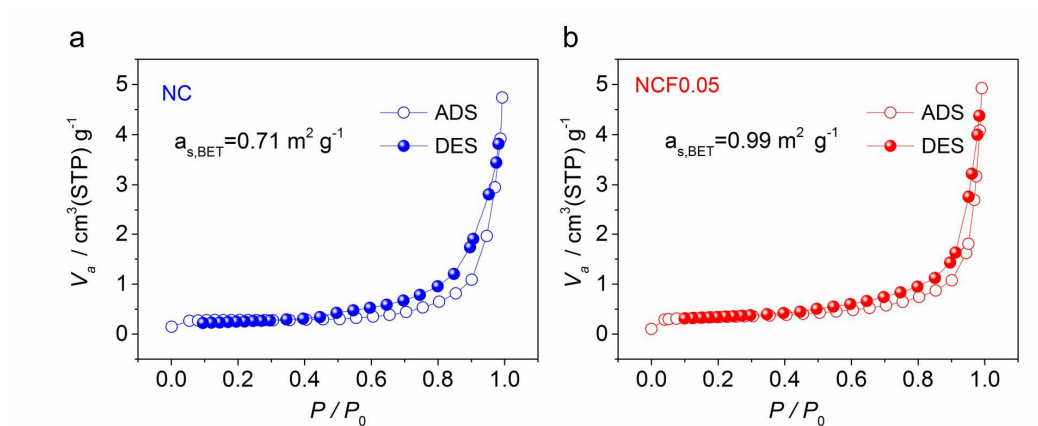


Figure S1 (a) Nitrogen adsorption-desorption isotherm curves of NC catalyst, suggesting that the BET surface area is $0.71 \text{ m}^2 \text{ g}^{-1}$. (b) Nitrogen adsorption-desorption isotherm curves of NCF0.05 catalyst, suggesting that the BET surface area is $0.99 \text{ m}^2 \text{ g}^{-1}$.

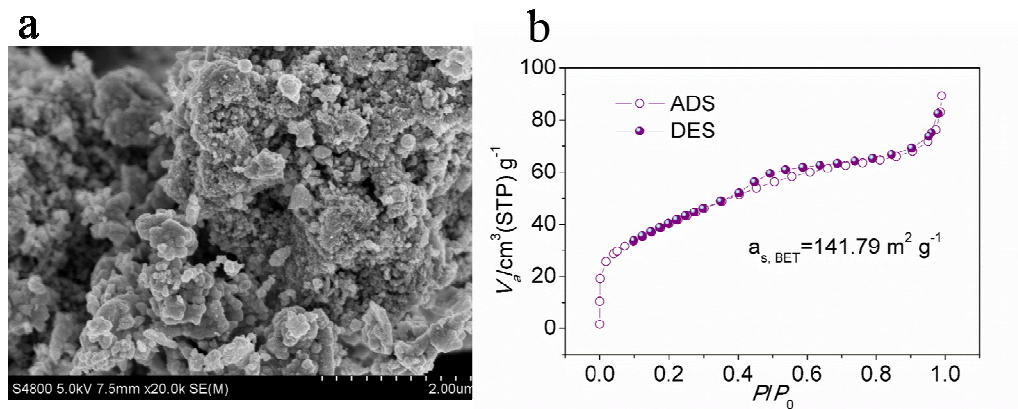


Figure S2 Properties of IrO_2 catalyst (Aladdin Industrial Corporation) (a) SEM image. (b) Nitrogen adsorption-desorption isotherm curves ($a_{s,\text{BET}} = 141.79 \text{ m}^2 \text{ g}^{-1}$).

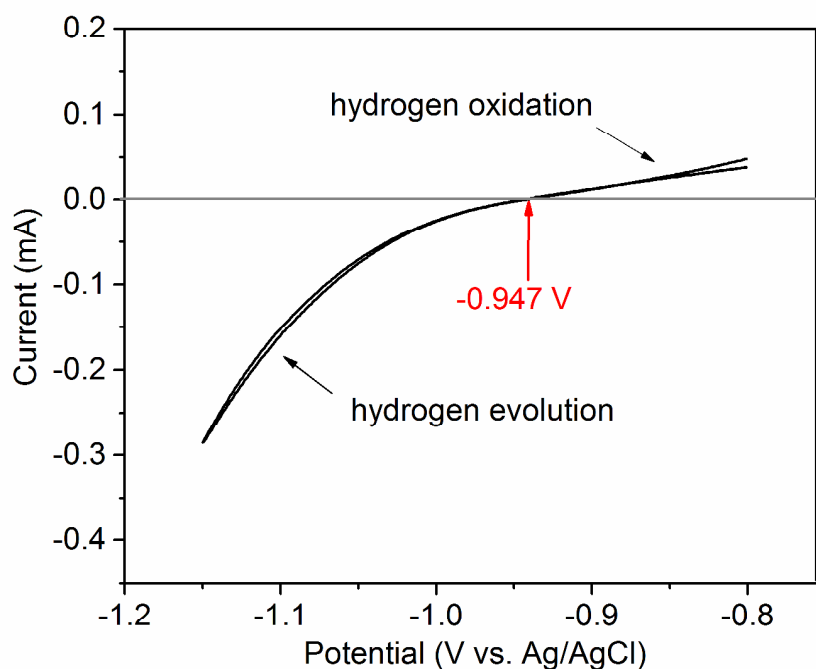


Figure S3 RHE calibration of the Ag/AgCl reference electrode in 0.1 M KOH. The calibration was performed on the working electrode of a platinum rotating disk electrode (PINE, 4 mm diameter, 0.126 cm²) in the high purity hydrogen-saturated 0.1 M KOH electrolyte. Cyclic voltammetry (CV) was run at a scan rate of 1 mV s⁻¹, and the average of the two potentials at which the current crossed over zero, which was approximately 0.947 V, was taken to be the thermodynamic potential for the hydrogen electrode reaction. In 0.1 M KOH solution, $E_{\text{RHE}} = E_{\text{Ag|AgCl}}(3.5 \text{ M KCl}) + 0.947 \text{ V}$, $\eta = E_{\text{RHE}} - 1.23 \text{ V} = E_{\text{Ag|AgCl}}(3.5 \text{ M KCl}) - 0.283 \text{ V}$.

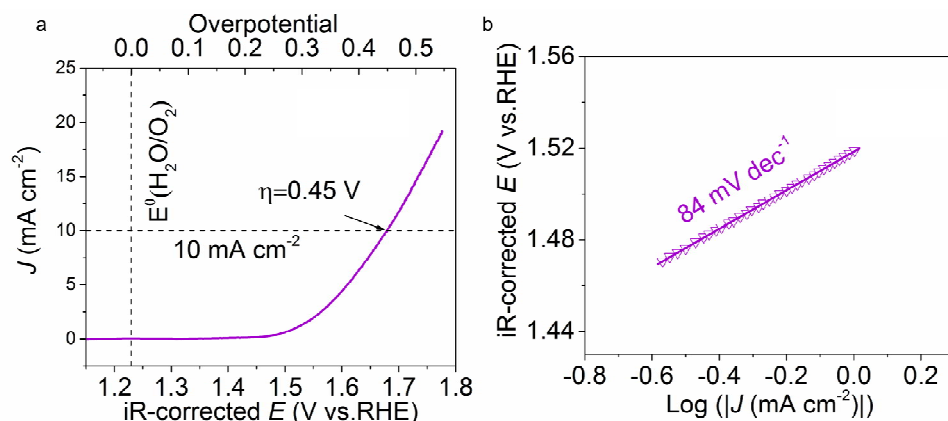


Figure S4 (a) OER polarization curves of IrO₂ with a scan rate of 5 mV s⁻¹ at the rotation speed of 1600 rpm in O₂-saturated 0.1 M KOH electrolyte on the RDE. (b) Corresponding Tafel plots.

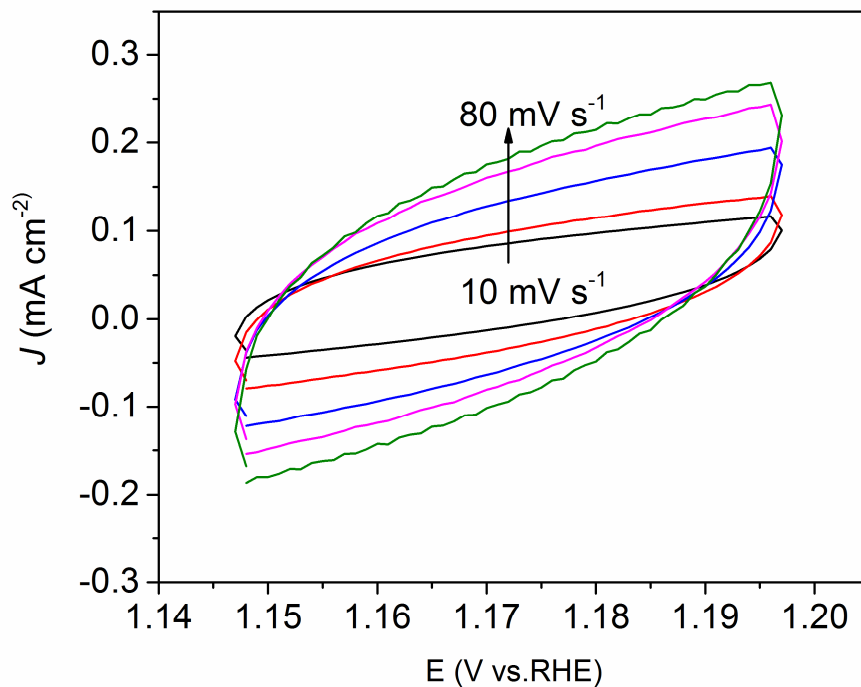


Figure S5 CV measurements in a non-faradic current region (1.147-1.197 V vs. RHE, no iR-corrected) at scan rates of 10, 20, 40, 60 and 80 mV s^{-1} for NC.

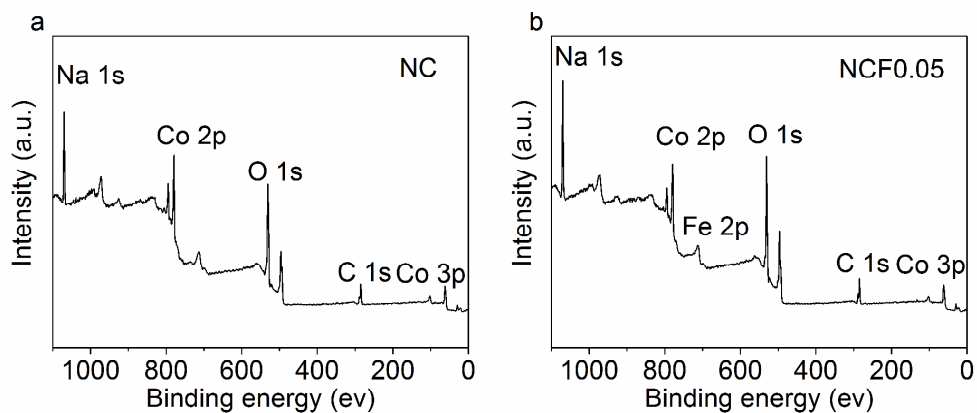


Figure S6 XPS survey spectra of as-obtained $\text{Na}_{0.86}\text{Co}_x\text{Fe}_{1-x}\text{O}_2$ electrocatalysts. a. NC powders, b. NCF0.05 powders.

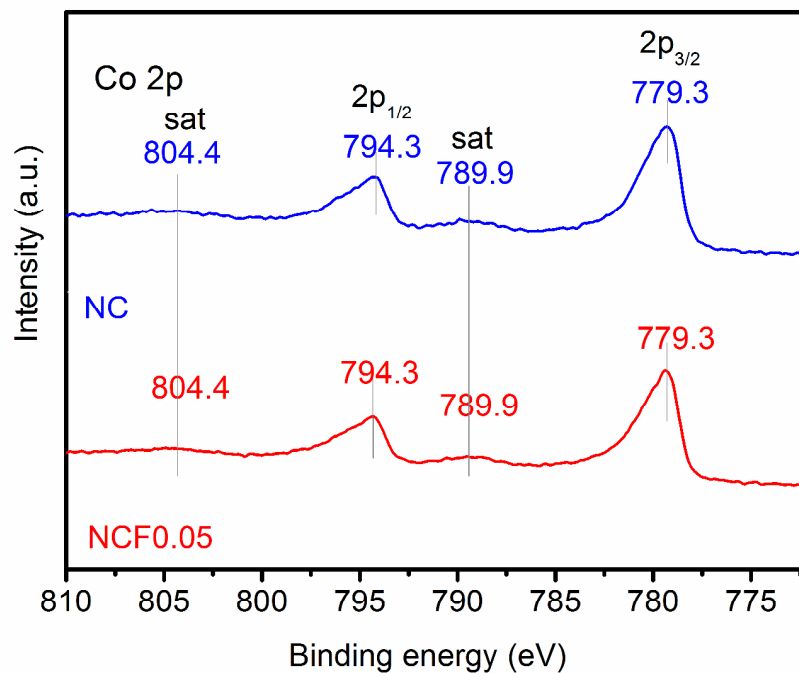


Figure S7 XPS Co 2p spectra of as-obtained $\text{Na}_{0.86}\text{Co}_x\text{Fe}_{1-x}\text{O}_2$ electrocatalysts.

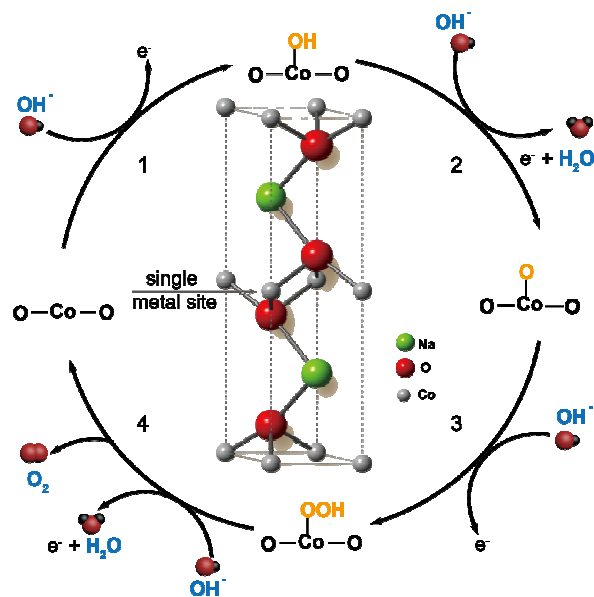


Figure S8 Schematic illustration of single-metal-site mechanism for OER on the surface of NC, where blue and yellow represents species in the solution and on the catalysts surface, respectively.

Table S1 Rietveld refinement results of NC and NCF0.05.

Sample	Structure	Space group	Lattice parameters			R_p	R_w	χ^2
			a(Å)	c(Å)	c/a			
NC	layered	P6 ₃ /mmc	2.8324	10.9439	3.864	1.45	2.50	1.45
NCF0.05	layered	P6 ₃ /mmc	2.8301	10.9937	3.885	1.26	2.56	1.26

Table S2 Bulk and surface compositions of as-prepared NC and NCF0.05 electrocatalysts in assistance of ICP-OES.

Nominal composition	Metal ions concentrations (mg L ⁻¹)			ICP-OES compositions
	Na	Co	Fe	
	NaCoO ₂	18.73	55.86	
NaCo _{0.95} Fe _{0.05} O ₂	18.83	53.03	2.66	Na _{0.86} Co _{0.95} Fe _{0.05} O ₂

Table S3 Comparison of catalytic activity of as-prepared NCF0.05 oxides towards OER with non-precious electrocatalysts.

Catalyst	Electrolyte	Overpotential (V)	Tafel slope (mV dec ⁻¹)	Refs.
NCF0.05	0.1 M KOH	0.45	60	This work
NC	0.1 M KOH	0.54	77	This work
LiCoO ₂	0.1 M KOH	0.43	83	1
CoFeO _x	0.1 M KOH	0.49	89	2
Fe doped nanocast Co ₃ O ₄	0.1 M KOH	0.49	N/A	3
CoFe ₂ O ₄ /biocarbon	0.1 M KOH	0.42	N/A	4
Microsphere NiCo ₂ O ₄ /rGO	0.1 M KOH	0.51	62	5
PNC/Co	1 M KOH	0.37	76	6
Mn ₃ O ₄ /CoSe ₂	0.1 M KOH	0.45	49	7
Nanocomposite CoO(OH)	0.1 M KOH	0.44	N/A	8
CoMnO	0.1 M KOH	0.43	N/A	9
O ₂ -BSCF	0.1 M KOH	0.42	130	10
nsLaNiO ₃ /NC	0.1 M KOH	0.43	42	11
NiCo ₂ O ₄ /G	0.1 M KOH	0.55	164	12
CoNP@NC-NG-800	0.1 M KOH	0.46	89	13
NiCo ₂ S ₄ @N/S-rGO	0.1 M KOH	0.47	N/A	14
Co _{0.5} Fe _{0.5} S@NMC	1 M KOH	0.41	159	15

Table S4 O 1s XPS peak deconvolution results

Electrocatalysts	Lattice O ²⁻	O ₂ ²⁻ /O ⁻	-OH/O ₂	H ₂ O/CO ₃ ²⁻
NC	32.06%	26.34%	26.19%	15.41%
NCF0.05	26.36%	30.49%	27.57%	15.58%

References

- (1) Zhu, Y.; Zhou, W.; Chen, Y.; Yu, J.; Liu, M.; Shao, Z., A High-Performance Electrocatalyst for Oxygen Evolution Reaction: LiCo_{0.8}Fe_{0.2}O₂. *Adv. Mater.* **2015**, *27*, 7150-7155.
- (2) Indra, A.; Menezes, P. W.; Sahraie, N. R.; Bergmann, A.; Das, C.; Tallarida, M.; Schmeißer, D.; Strasser, P.; Driess, M., Unification of Catalytic Water Oxidation and Oxygen Reduction Reactions: Amorphous Beat Crystalline Cobalt Iron Oxides. *J. Am. Chem. Soc.* **2014**, *136*, 17530-17536.
- (3) Grewe, T.; Deng, X.; Tüysüz, H., Influence of Fe Doping on Structure and Water Oxidation Activity of Nanocast Co₃O₄. *Chem. Mater.* **2014**, *26*, 3162-3168.
- (4) Liu, S.; Bian, W.; Yang, Z.; Tian, J.; Jin, C.; Shen, M.; Zhou, Z.; Yang, R., A Facile Synthesis of CoFe₂O₄/Biocarbon Nanocomposites as Efficient Bi-functional Electrocatalysts for the Oxygen Reduction and Oxygen Evolution Reaction. *J. Mater. Chem. A* **2014**, *2*, 18012-18017.
- (5) Umeshbabu, E.; Rajeshkhanna, G.; Justin, P.; Rao, G. R., NiCo₂O₄/rGO Hybrid Nanostructures for Efficient Electrocatalytic Oxygen Evolution. *J. Solid State Electrochem.* **2016**, *20*, 2725-2736.
- (6) Li, X.; Niu, Z.; Jiang, J.; Ai, L., Cobalt Nanoparticles Embedded in Porous N-Rich Carbon as an Efficient Bifunctional Electrocatalyst for Water Splitting. *J. Mater. Chem. A* **2016**, *4*, 3204-3209.
- (7) Gao, M.-R.; Xu, Y.-F.; Jiang, J.; Zheng, Y.-R.; Yu, S.-H., Water Oxidation Electrocatalyzed by an Efficient Mn₃O₄/CoSe₂ Nanocomposite. *J. Am. Chem. Soc.* **2012**, *134*, 2930-2933.
- (8) Subbaraman, R.; Tripkovic, D.; Chang, K.-C.; Strmcnik, D.; Paulikas, A. P.; Hirunsit, P.; Chan, M.; Greeley, J.; Stamenkovic, V.; Markovic, N. M., Trends in Activity for the Water Electrolyser Reactions on 3d M(Ni,Co,Fe,Mn) Hydr(oxy)oxide Catalysts. *Nat. Mater.* **2012**, *11*, 550-557.
- (9) Yeo, B. S.; Bell, A. T., Enhanced Activity of Gold-Supported Cobalt Oxide for the Electrochemical Evolution of Oxygen. *J. Am. Chem. Soc.* **2011**, *133*, 5587-5593.
- (10) Jung, J.-I.; Jeong, H. Y.; Kim, M. G.; Nam, G.; Park, J.; Cho, J., Fabrication of Ba_{0.5}Sr_{0.5}Co_{0.8}Fe_{0.2}O_{3-δ} Catalysts with Enhanced Electrochemical Performance by Removing an Inherent Heterogeneous Surface Film Layer. *Adv. Mater.* **2015**, *27*, 266-271.
- (11) Hardin, W. G.; Slanac, D. A.; Wang, X.; Dai, S.; Johnston, K. P.; Stevenson, K. J., Highly Active, Nonprecious Metal Perovskite Electrocatalysts for Bifunctional Metal–Air Battery Electrodes. *J. Phys. Chem. Lett.* **2013**, *4*, 1254-1259.
- (12) Lee, D. U.; Kim, B. J.; Chen, Z., One-Pot Synthesis of a Mesoporous NiCo₂O₄ Nanoplatelet and Graphene Hybrid and its Oxygen Reduction and Evolution

Activities as an Efficient Bi-functional Electrocatalyst. *J. Mater. Chem. A* **2013**, *1*, 4754-4762.

(13) Zhong, X.; Jiang, Y.; Chen, X.; Wang, L.; Zhuang, G.; Li, X.; Wang, J.-g., Integrating Cobalt Phosphide and Cobalt Nitride-Embedded Nitrogen-Rich Nanocarbons: High-Performance Bifunctional Electrocatalysts for Oxygen Reduction and Evolution. *J. Mater. Chem. A* **2016**, *4*, 10575-10584.

(14) Liu, Q.; Jin, J.; Zhang, J., NiCo₂S₄@graphene as a Bifunctional Electrocatalyst for Oxygen Reduction and Evolution Reactions. *ACS Appl. Mater. Interfaces* **2013**, *5*, 5002-5008.

(15) Shen, M.; Ruan, C.; Chen, Y.; Jiang, C.; Ai, K.; Lu, L., Covalent Entrapment of Cobalt–Iron Sulfides in N-Doped Mesoporous Carbon: Extraordinary Bifunctional Electrocatalysts for Oxygen Reduction and Evolution Reactions. *ACS Appl. Mater. Interfaces* **2015**, *7*, 1207-1218.